

Dalton Transactions

Accepted Manuscript



This is an *Accepted Manuscript*, which has been through the Royal Society of Chemistry peer review process and has been accepted for publication.

Accepted Manuscripts are published online shortly after acceptance, before technical editing, formatting and proof reading. Using this free service, authors can make their results available to the community, in citable form, before we publish the edited article. We will replace this *Accepted Manuscript* with the edited and formatted *Advance Article* as soon as it is available.

You can find more information about *Accepted Manuscripts* in the [Information for Authors](#).

Please note that technical editing may introduce minor changes to the text and/or graphics, which may alter content. The journal's standard [Terms & Conditions](#) and the [Ethical guidelines](#) still apply. In no event shall the Royal Society of Chemistry be held responsible for any errors or omissions in this *Accepted Manuscript* or any consequences arising from the use of any information it contains.

Stepwise assembly of a molecular box from 16-electron half-sandwich precursor [Cp*M(pdt)] (M = Rh, Ir)

Cite this: DOI: 10.1039/x0xx00000x

Jing-Jing Liu,^a Yue-Jian Lin^a and Guo-Xin Jin^{*a}Received 00th January 2012,
Accepted 00th January 2012

DOI: 10.1039/x0xx00000x

www.rsc.org/

The coordinatively-unsaturated 16-electron half-sandwich precursors [Cp*M(pdt)] (M = Rh, Ir; pdt = pyrazine-2,3-dithiol) have been synthesized. X-ray crystallography in combination with ¹H NMR analysis were used to elucidate the nature of the precursors. The Rh(III) precursor displays a dimeric form in *trans* arrangement in the solid state, formulated as [(Cp*Rh)₂(μ(S)-pdt)₂] (**1**), in which covalent Rh-S bonds bridge the metal centers. In solution, however, dimers **1** and monomers **2** coexist in equilibrium. The dissociation equilibrium of **1** in DMSO-*d*₆ was evaluated by ¹H NMR at several temperatures between 20–80 °C. The Ir(III) precursor [Cp*Ir(pdt)] (**3**) is monomeric form, and stable in the solid state and solution. Due to their unsaturation and bridging properties, these precursors were further used in stepwise assembly reactions with the binuclear building blocks to give open macrocycles and a closed molecular box.

Introduction

Metal-dithiolene complexes have generated considerable interest as a new class of materials used in electromagnetic systems¹ and molecular devices.² Particularly, dithiolene ligands have great potential as ancillary groups in the rational design of polymetallic complexes, due to their coordinative unsaturation in planar MS₂C₂ subunits.^{3,4} Besides their strong tendency to undergo addition reactions with electron donors at the metal centers, they exhibit suitable attributes for the design of a variety of novel coordination motifs.⁵ Although much work has been devoted to this topic, there are very few reports focusing on the rational design of organometallic macrocycles and cages supported by coordinatively-unsaturated 16-electron subunits.⁶

Our efforts have been focused on finding functional ligands suitable for the construction of organometallic macrocycles and cages.^{7,8} Reliable approaches have been exploited based on metal-based subunits, which allow step-by-step syntheses because of different reactivity of various functionalities.⁹ In this regard, it is important to mention that the pyrazine-2,3-dithiol

ligand (H₂pdt), has been widely used in the construction of molecular conductors.¹⁰ However, due to the nature of dithiolene ligand, it appeared possible that the pdt dianion could chelate {Cp*M} (M = Rh and Ir, Cp* = pentamethylcyclopentadienyl) fragments, giving 16-electron half-sandwich species.^{11,12} Meanwhile, such ligands can act as bridging elements through the nitrogen atoms of adjoined pyrazine moieties (see Fig. 1). Therefore, it should be possible to control the molecular arrangement, giving rise to multinuclear assemblies.

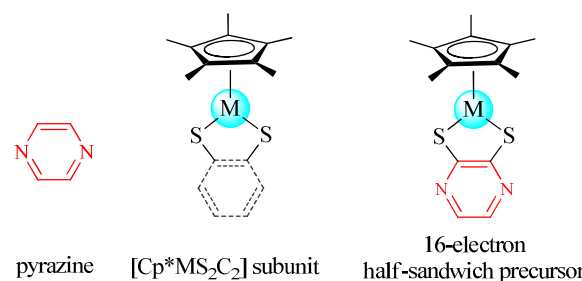


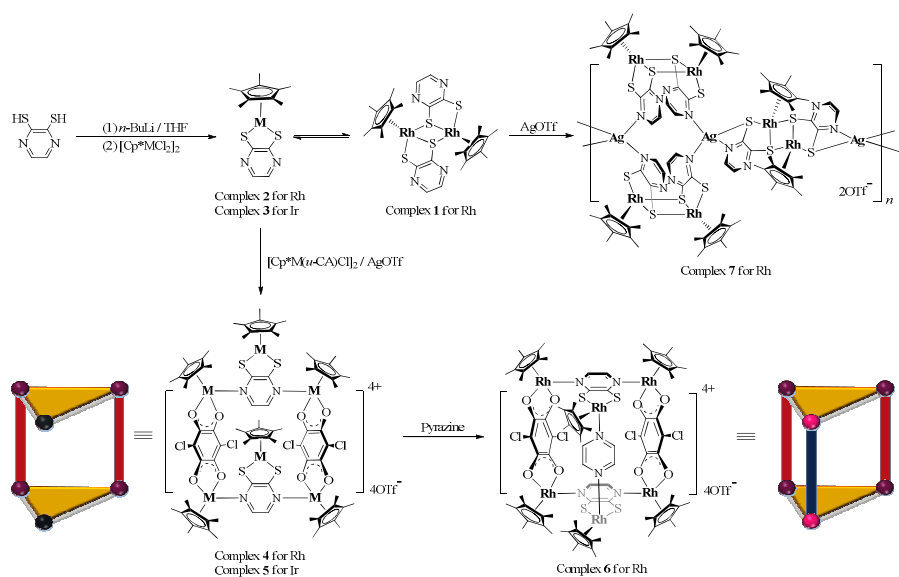
Figure 1 16-electron half-sandwich precursor [Cp*M(pdt)] in active site model (M = Rh and Ir).

Herein we report the synthesis of representative 16-electron half-sandwich precursors [Cp*M(pdt)] (M = Rh and Ir). The Rh(III) complex is a dimer featuring a *trans* arrangement of the Cp* ligands relative to the Rh-Rh vector in the solid state, formulated as [(Cp*Rh)₂(μ(S)-pdt)₂] (**1**). Complex **1** dissociates in solution, thus dimers **1** and monomers **2** coexist in equilibrium, which was evaluated by ¹H NMR at several

^aShanghai Key Laboratory of Molecular Catalysis and Innovative Material, Department of Chemistry, Fudan University, Shanghai, 200433, P. R. China. E-mail: gxinjin@fudan.edu.cn; Fax: (+86)-21-65643776.

Dedicated to Professor Ekkehardt Hahn on the occasion of his 60th birthday

† Electronic Supplementary Information (ESI) available: CCDC No. 1045350 (**1**), 1045351 (**3**), 1045352 (**4**), 1045353 (**5**), 1045354 (**6**) and 1045355 (**7**) contain the supplementary crystallographic data for this paper. See <http://dx.doi.org> for crystallographic data in CIF or other electronic format.



Scheme 1 Synthetic routes to complexes 1-7.

temperatures between 20-80 °C. For the Ir(III) complex, $[\text{Cp}^*\text{Ir}(\text{pdt})]$ (**3**) exists in the 16-electron monomeric form, and is stable in the solid state and solution. Following a stepwise strategy, starting from the 16-electron half-sandwich precursors, a series of the macrocycles featuring a coordinatively unsaturated metal center in two opposite bridging groups ($M = \text{Rh}$ (**4**) and $M = \text{Ir}$ (**5**)) have been synthesized. Most interestingly, in solution, by introduction of the pyrazine, these are linked converting the hexanuclear macrocycle **4** into a distorted trigonal-prism **6**. In addition, complex **7** is a 1D heterometallic framework structure supported by $[(\text{Cp}^*\text{Rh})_2(\mu(\text{S})\text{-pdt})]$ dimeric units in *cis* and *trans* arrangement. Therefore, for the first time, we demonstrate the extension of 16-electron half-sandwich precursors as building blocks in the construction of organometallic macrocycles and cages.

Results and discussion

Synthesis and characterization

As shown in **Scheme 1**, treatment of pyrazine-2,3-dithiol with two molar equivalents of *n*-BuLi in THF at -78 °C, followed by the addition of 0.5 molar equivalents of $[(\text{Cp}^*\text{MCl}_2)_2]$ ($M = \text{Rh}$ and Ir), results in displacement of the chlorides from the M^{III} centers and a dimer formulated as $[(\text{Cp}^*\text{Rh})_2(\mu(\text{S})\text{-pdt})_2]$ (**1**) in 68% yield, while a similar reaction give the expected mononuclear precursor $[\text{Cp}^*\text{Ir}(\text{pdt})]$ (**3**) (Yield: 31%). However, in solution, complex **1** partially dissociates, giving the 16-electron monomeric complex, $[\text{Cp}^*\text{Rh}(\text{pdt})]$ (**2**), giving an equilibrium of dimers **1** and monomers **2**. Compared to nitrogen or oxygen ligands, the reactions to form the 16-electron half-sandwich precursors occur more rapidly, since the softer pdt dianion is a better ligand towards $\{\text{Cp}^*\text{M}\}$ ($M = \text{Rh}$ and Ir) fragments.

As illustrated in Fig. S1, the ^1H NMR spectra of complex **1** in CDCl_3 shows one complete set of proton resonances for the pdt ligands and the Cp^* rings, as evidenced by two signals at δ 7.89 and 7.77 ppm, peaks assignable to the pdt protons, along with one singlet peak at δ 1.32 ppm for the methyl protons of the Cp^* rings. These proton signals are consistent with the formation of the dimeric complexes. However, additional smaller peaks also exist: the peaks attributable to the pdt ligands and the Cp^* rings appear at δ 8.26 ppm and δ 1.97 ppm, we assume that these species correspond to a mononuclear complex, $[\text{Cp}^*\text{Rh}(\text{pdt})]$ (**2**). The ESI-MS spectrum of **1** shows an isotopic distribution corresponding to $[(\text{Cp}^*\text{Rh})_2(\mu(\text{S})\text{-pdt})_2]^+$ ($M = 760.98$) at $m/z = 760.98$ (see Fig. S2). In comparison with those of complex **3**, it is stable in solution, no dimerization reaction is observed in the ^1H NMR spectra, only one single peak at δ 2.13 ppm for methyl protons of the Cp^* ligand and one peak at δ 8.23 ppm for pdt dianion protons are observed in CDCl_3 . Additionally, the ESI-MS spectrum of **3** indicates the existence of the mononuclear ion $[\text{Cp}^*\text{Ir}(\text{pdt})]^+$ ($m/z = 471.05$) (see Fig. S4 and S5).

Due to their unsaturation and bridging properties, it was envisaged that fine tuning of the geometry and functionality of new metal-dithiolene organometallic macrocycles or cages could be achieved. When the known bridging binuclear complexes $[\text{Cp}^*_2\text{M}_2(\mu\text{-CA})\text{Cl}_2]$ ¹³ ($M = \text{Rh}, \text{Ir}$; $\mu\text{-CA} = 2,5\text{-dichloro-3,6-dihydroxy-1,4-benzoquinone}$) were used along with the 16-electron precursors in a 1:0.5 and 1:1 ratio (with addition of silver salts), the open hexanuclear organometallic macrocycles $\{\text{Cp}^*_2\text{M}_2(\mu\text{-CA})[\text{Cp}^*\text{M}(\text{pdt})]\}_2 \cdot (\text{OTf})_4$ ($M = \text{Rh}$ (**4**) and $M = \text{Ir}$ (**5**)) were obtained in about 63% and 42% yields, respectively. Interestingly, utilizing the coordinative unsaturation of **4**, we further tuned the open rectangular macrocycle **4** by adding pyrazine in a 1:1 ratio in methanol, resulting in the 18-electron closed box $\{\text{Cp}^*_2\text{Rh}_2(\mu\text{-CA})[\text{Cp}^*\text{Rh}(\text{pdt})]\}_2(\text{pyrazine}) \cdot (\text{OTf})_4$ (**6**) in 37% yield.

Additionally, complex $\{[\text{Ag}(\text{Cp}^*\text{Rh})_3(\text{pdt})_3] \cdot (\text{OTf})\}_n$ (**7**) was obtained from dimeric **1** in the presence of AgOTf (Yield: 30%).

Molecular Structures

The dinuclear form of complex **1** ($M = \text{Rh}$) was confirmed by single-crystal X-ray diffraction analysis. It crystallized in the monoclinic space group $P2(1)/c$. In Fig. 2(a), the pdt dianion acts both as a chelating ligand via the S1 and S2 atoms and as a bridging one through the S2 atom. The distance between two Rh atoms in the dimer is 3.549(7) Å, which indicates no bonding interaction between them. Due to the dimeric form of the complex, the ligand sphere around both Rh centers satisfies the 18-electron rule, and the dimer form is thereby stable in the solid state. However, compared to the Rh-S1 (2.352(16) Å) and Rh-S2 (2.354(16) Å) distances, the bond lengths between the Rh atoms and the bridging S2 atoms are significantly longer (2.401(15) Å). This elongation appears to cause easy cleavage of the S-bridge in solution, giving the mononuclear form. The Rh center in the monomer, with 16 valence electrons, is coordinatively unsaturated. The monomeric complex $[\text{Cp}^*\text{Rh}(\text{pdt})]$ (**2**) could not be isolated, but was characterized by ^1H NMR.

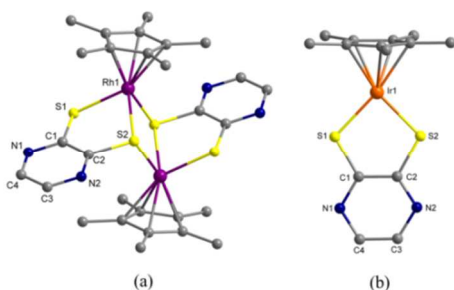


Figure 2 Crystallographically-determined molecular structures of $[(\text{Cp}^*\text{Rh})_2(\mu(\text{S})\text{-pdt})_2]$ (**1**) (a) and $[\text{Cp}^*\text{Ir}(\text{pdt})]$ (**3**) (b). H atoms have been omitted for clarity (violet for Rh, orange for Ir, yellow for S, blue for N, gray for C).

X-ray structural analysis reveals that complex **3** is a monomer. It is crystallized in the orthorhombic space group $Pca2(1)$. As displayed in Fig. 2(b), **3** is a coordinatively-unsaturated five-coordinate species with Ir center. However, in order to achieve an 18 valence electron configuration for the Ir(III) center, the thiolate ligand donates p -electron density to the metal, and consequently, the Ir-S bonds have a formal bond order of 1.5.¹¹ Accordingly, the Ir-S bond lengths are 2.257(21) (Ir-S1) and 2.248(19) (Ir-S2) Å, significantly shorter than the normal Ir-S bond length (2.35 Å),¹⁴ or the Rh-S bond lengths (Rh-S1 2.352(16) and Rh-S2 2.354(16) Å) in complex **1**. Notably, both the electronic and metal center reasons are responsible for the formation of complex **3** as monomer. Due to the p -electron donation from the S atoms, the Ir atom is almost coplanar with the chelated pdt dianion in **3**, which is in contrast to the non-planar structure of complex **1**.

Complexes **4** and **5** may be described as open hexanuclear rectangular macrocycles constructed from μ -CA units and 16-electron precursors (see Fig. 3). Complex **4** crystallized in the monoclinic space group $P2(1)/c$. As shown in Fig. S6, $\{\text{Cp}^*\text{Rh}\}$ and $\{\text{Cp}^*\text{Rh}\}_2$ fragments all adopt a classical three-legged piano-stool geometries in which the Rh centers are coordinated by two $\text{O}_{\mu\text{-CA}}$ atoms and one N_{pdt} atom. Four $\{\text{Cp}^*\text{Rh}\}$ vertices reside on the edges of the rectangular structure with distances of 8.048(18) (Rh1–Rh2) and 7.021(21) (Rh1–Rh2A) (A 1-x, 1-y, -z) Å, respectively. The dihedral angles between the μ -CA units and the 16-electron precursors in the rectangular macrocycle **4** are 87.7°. However, coordinatively unsaturated metal center are in two opposite bridging groups. Similarly, as shown in Fig. S7, complex **5** also shows an open rectangular macrocycle with Ir atoms. The distances between the adjacent Ir atoms are 8.069(12) (Ir1–Ir2) and 6.993(16) (Ir1–Ir2A) (A-x, 1-y, 2-z) Å, respectively. The dihedral angles between the μ -CA units and the 16-electron precursors in the rectangular macrocycle **5** are 87.5°. It is noteworthy that, ^1H NMR showed two complete sets of proton resonances for the open macrocycles, suggesting that *cis* and *trans* conformations coexist in solution for the complexes **4** and **5**. The major features of the complex **4** in *trans* arrangement are signals from the pdt ligand (δ 7.93 ppm), the 16-electron Cp^* fragments (δ 2.07 ppm), and the 18-electron Cp^* fragments (δ 1.67 ppm), respectively. For complex **4** in *cis* arrangement, the corresponding signals appear at δ 8.09 ppm, δ 2.02 ppm and δ 1.68 ppm, respectively. It is noteworthy that there is inconversion between *cis* and *trans* arrangements in **4** (see Fig. S9). The spectral data of complex **5** is qualitatively very similar to complex **4** (see Fig. S8 and S10).

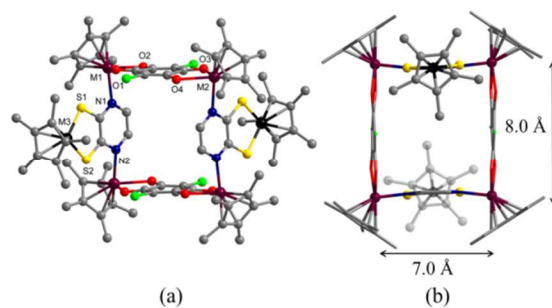


Figure 3 (a) Crystallographically-determined molecular structures of $\{\text{Cp}^*_2\text{M}_2(\mu\text{-CA})[\text{Cp}^*\text{M}(\text{pdt})]\}_2 \cdot (\text{OTf})_4$ ($M = \text{Rh}$ (**4**) and $M = \text{Ir}$ (**5**)). H atoms, anions, and solvent molecules have been omitted for clarity; (b) Simplified view of **4** and **5** in wireframe mode (Dark red for M1 and M2, Black for M3, yellow for S, blue for N, red for O, gray for C, green for Cl).

We reasoned that 16-electron unsaturated building blocks might provide a method for the formation of a closed molecular box through the use of linear bidentate ligands. Using this logic, we have successfully transformed the open rectangular macrocycle **4** into the 18-electron trigonal-prism **6** using a pyrazine bridging ligand as a “lid” for the box. X-ray structural analysis reveals that complex **6** is a hexanuclear cage,

crystallized in the monoclinic space group $C2/C$. As shown in Fig. 4, all of the Rh atoms show three-legged piano-stool geometries, in which Rh1 and Rh2 are both coordinated by O_2N donor sets and one Cp^* fragment, while the Rh3 atoms are bound instead by S_2N donor sets. The pyrazine bridged Rh3-Rh3 distance is 7.082(10) Å, and the distances of between adjacent Rh atoms along the edges of rectangular box are 8.037(14) (Rh1-Rh2) and 6.989(17) (Rh1-Rh2A) (A 2-x, y, 1.5-z) Å, respectively. In the cage **6**, the dihedral angles of the 16-electron precursors with the μ -CA units and the pyrazine ligands are 89.6 and 86.3°, respectively. As shown in Fig. S11, the 1H NMR spectrum of **6** consists of two single peaks at δ 8.49 ppm and δ 7.41 ppm corresponding to the pyrazine and pdt ligands, respectively, and at δ 1.75 ppm and δ 1.77 ppm corresponding to Cp^* fragments, respectively. These proton signals are consistent with the formation of the closed box.

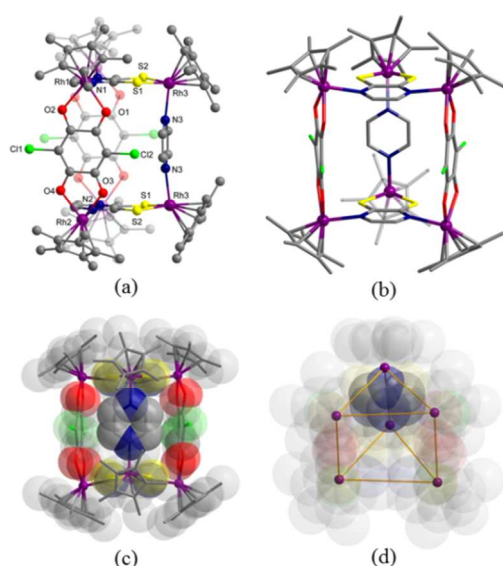


Figure 4 (a) Crystallographically-determined molecular structure of $\{Cp^*_2Rh_2(\mu\text{-CA})[Cp^*Rh(pdt)]_2(\text{pyrazine})\cdot(\text{OTf})_4$ (**6**). H atoms, anions, and solvent molecules have been omitted for clarity; (b) Simplified view of **6** in wireframe mode; (c) View of **6** in space-filling mode; (d) Perspective image showing the closed box of **6** (violet for Rh, yellow for S, blue for N, red for O, gray for C, green for Cl).

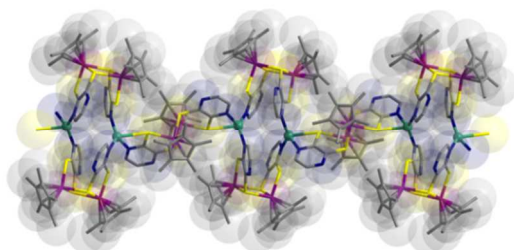


Figure 5 Crystallographically-determined molecular structure of $[Ag(Cp^*Rh)_3(pdt)_3]\cdot(\text{OTf})_n$ (**7**). H atoms, anions and solvent molecules have been omitted for clarity (violet for Rh, yellow for S, blue for N, red for O, gray for C, sea green for Ag).

Complex **7** is a 1D coordination polymer consisting of silver-bridged $[(Cp^*Rh)_2(\mu(S)\text{-pdt})_2]$ dimers in *cis*- and *trans*- modes (see Fig. 5). The fundamental silver(I) coordination environment in **7** is depicted in Fig. S12. The silver atom adopts a tetrahedral geometry, coordinated by two N_{pdt} atoms (N_3, N_5) from two *cis* dimers, and one N_{pdt} atom (N_2) and one S atom (S_2) from a *trans* dimer. The $Ag\cdots Ag$ distances spanned by *cis* and *trans* dimers are 4.387(9) and 10.940(10) Å, respectively. Importantly, it also represents the first example of the coexistence of *cis* and *trans* dimers of **1** in the solid state (see Fig. S13).

Dissociation equilibrium in solution

The Rh^{III} dimer **1** and monomer **2** coexist in equilibrium, while in the solid state **1** exists in its dimeric form. The dissociation equilibrium of **1** in solution,^{11,15} was studied by 1H NMR spectra in $DMSO-d_6$ at several temperatures between 20 and 80 °C, as shown in Fig. 6(a). The set of signals for **2** (in red) grow gradually with increasing temperature, while those of **1** (in blue) decrease in intensity. A similar intense change was observed in $CDCl_3$ (see Fig.S3). However, the peaks for **2** in $DMSO-d_6$ change relatively large with temperature in contrast to $CDCl_3$, which is probably associated with the solvent-dependent. Presumably, DMSO has the ability to donate an electron pair, which could stabilize monomer with 16-electrons. In addition, the equilibrium constant, $K = [2]^2/[1]$, is determined by the monomer and dimer ratio. Dissociation enthalpies (ΔH) and entropies (ΔS) were evaluated from the slope and intercept of the Van't Hoff plots of $\ln K$ vs $1/T$ (see Fig. 6(b)). The values of ΔH and ΔS were obtained as 32 kJ mol^{-1} and 91 $\text{J K}^{-1} \text{mol}^{-1}$ in $DMSO-d_6$, respectively. In contrast, iridium complex **3** is stable in solution and no dimerization reaction was observed.

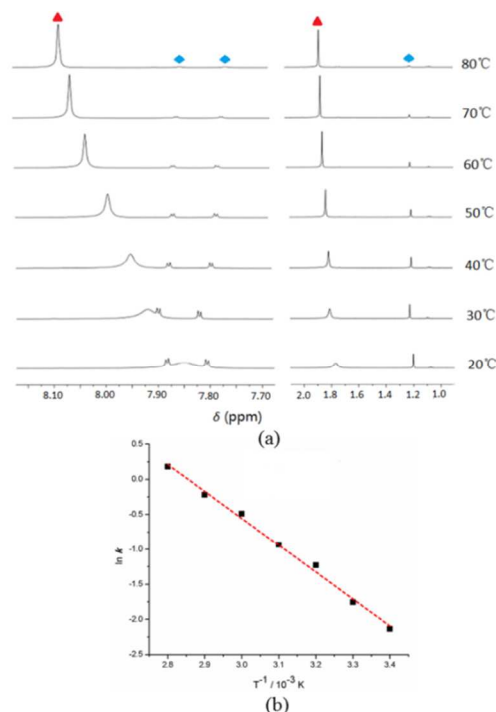


Figure 6 (a) ^1H NMR spectral change of complexes **1** (blue) and **2** (red) in $\text{DMSO-}d_6$ with increasing temperature between 20-80 $^\circ\text{C}$; (b) Van't Hoff plots of $\ln K$ vs $1/T$ for the equilibrium between **1** and **2**.

Conclusions

In summary, 16-electron half-sandwich precursors, the dimer $[(\text{Cp}^*\text{Rh})_2(\mu(\text{S})\text{-pdt})_2]$ (**1**) and the monomer $[\text{Cp}^*\text{M}(\text{pdt})]$ ($\text{M} = \text{Rh}$ (**2**) and Ir (**3**)), have been synthesized and characterized. The reactivity of these 16-electron half-sandwich precursors was investigated. In solution, dimer **1** dissociates to the monomer **2**, as determined by variable-temperature ^1H NMR in $\text{DMSO-}d_6$ between 20-80 $^\circ\text{C}$. The potential of these precursors to function as metal-based subunits in formation of organometallic macrocycles and cages is demonstrated. These results may be useful for further work on metal-dithiolate complexes in the design of organometallic materials.

Experimental Section

General considerations. All reactions were carried out under a nitrogen atmosphere by using standard Schlenk techniques. All of the solvents were freshly distilled prior to use. THF was distilled under nitrogen from sodium benzophenone and MeOH was distilled over Mg/I_2 . The starting materials $[(\text{Cp}^*\text{MCl}_2)_2]^{16}$ ($\text{M} = \text{Rh}$ and Ir) and pyrazine-2,3-dithiol 10 (H_2pdt) and $[\text{Cp}^*_2\text{M}_2(\mu\text{-CA})\text{Cl}_2]^{13}$ ($\text{M} = \text{Rh}$ and Ir) were prepared according to reported procedures, respectively. Elemental analyses were performed on an Elementar III Vario EI analyzer. ^1H NMR (400/500 MHz) spectra were obtained on a Bruker DMX-400/500 spectrometer. IR spectra of the solid samples (KBr tablets) in the range 400-4000 cm^{-1} were measured on a Nicolet Avatar-360 spectrophotometer. ESI-MS spectra were recorded on a Micro TOF II mass spectrometer using electrospray ionization.

Synthesis of 1. Yellow suspension of H_2pdt (28.8 mg, 0.20 mmol) in THF (20 mL) was treated by addition of 2 equiv. of *n*-BuLi at -78 $^\circ\text{C}$. To the solution was added $[\text{Cp}^*\text{RhCl}_2]_2$ (62.0 mg, 0.10 mmol) with stirring at room temperature, and the colour turned red immediately. The mixture was stirred for 24h, after concentrating to get a dark red solid, which was extracted by dichloromethane, and further washed by diethyl ether and dried under vacuum. Yield: 51.7 mg, 68%. Crystals of **1** suitable for an X-ray diffraction study were obtained by slow diffusion with diethyl ether and THF. Anal. Calcd (%) for $\text{C}_{28}\text{H}_{34}\text{N}_4\text{S}_4\text{Rh}_2$: C 44.21, H 4.51, N 7.37. Found: C 43.93, H 4.68, N 7.10. ESI-MS: m/z calcd for I^+ : 760.98, found: 760.98. IR (KBr disk): 3076(w), 3026(w), 2964(w), 2905(w), 2849(w), 1633(m), 1476(m), 1412(w), 1374(m), 1315(s), 1280(m), 1277(m), 1262(m), 1145(vs), 1056(m), 1027(s), 800(m), 640(w), 587(w), 452(w) cm^{-1} . ^1H NMR (400MHz, CDCl_3 , ppm): δ 7.89 (d, 2H, $J = 2.4$, pdt), δ 7.77 (d, 2H, $J = 2.4$, pdt), δ 1.32 (s, 30H, Cp*).

For the mononuclear complex **2**, which exists in solution. ^1H NMR (400MHz, CDCl_3 , ppm): δ 8.26 (s, 2H, pdt), δ 1.97 (s, 15H, Cp*).

Synthesis of 3. A procedure similar to that utilized in the synthesis of **1** was used, except $[\text{Cp}^*\text{RhCl}_2]_2$ was replaced by $[\text{Cp}^*\text{IrCl}_2]_2$. Yield: 29.1 mg, 31%. Slow evaporation of **3** in the mixed solvent (methanol and dichloromethane) in the air produced red crystals suitable for X-ray study. Anal. Calcd (%) for $\text{C}_{14}\text{H}_{17}\text{N}_2\text{S}_2\text{Ir}$: C 35.80, H 3.65, N 5.96. Found: C 35.63, H 3.56, N 5.90. ESI-MS: m/z calcd for 3^+ : 471.05, found: 471.05. IR (KBr disk): 3043(w), 3011(w), 2961(w), 2919(m), 2850(w), 1634(w), 1455(m), 1383(m), 1326(s), 1292(m), 1165(vs), 1120(w), 1071(w), 1028(m), 852(w), 722(w), 696(w), 542(w) cm^{-1} . ^1H NMR (400MHz, CDCl_3 , ppm): δ 8.23 (s, 2H, pdt), δ 2.13 (s, 15H, Cp*).

Synthesis of 4. A mixture of $[\text{Cp}^*_2\text{Rh}_2(\mu\text{-CA})\text{Cl}_2]$ (22.6 mg, 0.03 mmol) and AgOTf (15.4 mg, 0.06 mmol) in methanol (6 mL) was stirred at room temperature for 5h. After filtration to remove AgCl, **1** (11.4 mg, 0.015 mmol) was added to the filtrate, and the mixture was stirred for 24h. Then the solution was concentrated to give a dark red solid, which was washed by diethyl ether and dried under vacuum. Yield: 25.8 mg (63%). X-ray quality crystals for **4** were obtained by slow diffusion of diethyl ether into methanol. Anal. Calcd (%) for $\text{C}_{84}\text{H}_{94}\text{N}_4\text{O}_{20}\text{S}_8\text{Cl}_4\text{F}_{12}\text{Rh}_6$: C 37.05, H 3.48, N 2.06. Found: C 37.23, H 3.55, N 2.12. IR (KBr disk): 2981(w), 2925(w), 2360(w), 2342(w), 1620(w), 1514(s), 1497(s), 1430(w), 1374(s), 1259(s), 1224(w), 1192(w), 1162(m), 1083(w), 1068(w), 1031(m), 856(w), 839(w), 639(m), 574(w) cm^{-1} . ^1H NMR (400MHz, CD_3OD , ppm): δ 8.09 (s, 4H, pdt, *cis*), δ 7.93 (s, 4H, pdt, *trans*), δ 2.07 (s, 30H, Cp*, *trans*), δ 2.02 (s, 30H, Cp*, *cis*), δ 1.68 (s, 60H, Cp*, *cis*), δ 1.67 (s, 60H, Cp*, *trans*).

Synthesis of 5. A mixture of $[\text{Cp}^*_2\text{Ir}_2(\mu\text{-CA})\text{Cl}_2]$ (28.0 mg, 0.03 mmol) and AgOTf (15.4 mg, 0.06 mmol) in methanol (6 mL) was stirred at room temperature for 5h. After filtration to remove AgCl, **3** (14.1 mg, 0.03 mmol) was added to the filtrate, and the mixture was stirred for 24h. Then the solution was concentrated to give a dark red solid, which was washed by diethyl ether and dried under vacuum. Yield: 20.5 mg (42%). X-ray quality crystals for **5** were obtained by slow diffusion of diethyl ether into methanol. Anal. Calcd (%) for $\text{C}_{84}\text{H}_{94}\text{N}_4\text{O}_{20}\text{S}_8\text{Cl}_4\text{F}_{12}\text{Ir}_6$: C 30.95, H 2.91, N 1.72. Found: C 30.83, H 2.86, N 1.65. IR (KBr disk): 2988(w), 2922(w), 1624(w), 1504(s), 1451(s), 1373(s), 1316(w), 1261(s), 1224(w), 1192(w), 1168(m), 1079(w), 1065(w), 1031(m), 868(w), 846(w), 639(m), 573(w) cm^{-1} . ^1H NMR (400MHz, CD_3OD , ppm): δ 8.12 (s, 4H, pdt, *cis*), δ 7.96 (s, 4H, pdt, *trans*), δ 2.18 (s, 30H, Cp*, *trans*), δ 2.13 (s, 30H, Cp*, *cis*), δ 1.61 (s, 60H, Cp*, *cis*), δ 1.61 (s, 60H, Cp*, *trans*).

Synthesis of 6. To the solution of **4** (27.2 mg, 0.01 mmol) in methanol was added pyrazine (0.8 mg, 0.01 mmol) with stirring for 24h. Then the solution was concentrated to give a dark red solid, which was washed by diethyl ether and dried under vacuum. Yield: 10.4 mg (37%). X-ray quality crystals for **6** were obtained by slow diffusion of diethyl ether into methanol. Anal. Calcd (%) for $\text{C}_{88}\text{H}_{98}\text{N}_6\text{O}_{20}\text{S}_8\text{Cl}_4\text{F}_{12}\text{Rh}_6$: C 37.70, H 3.52, N 3.00. Found: C 37.59, H 3.44, N 2.92. IR (KBr disk): 2970(w), 2924(w), 2360(w), 2342(w), 1630(w), 1518(s), 1501(s), 1424(w), 1376(s), 1260(s), 1224(w), 1161(m),

1109(w), 1080(w), 1031(m), 859(w), 842(w), 812(w), 639(m), 574(w) cm^{-1} . $^1\text{H NMR}$ (400MHz, CD_3OD , ppm): δ 8.49 (s, 4H, pyrazine), δ 7.41 (s, 4H, pdt), δ 1.77 (s, 30H, Cp*), δ 1.75 (s, 60H, Cp*).

Synthesis of 7. Excess AgOTf (36.0 mg, 0.14 mmol) was added into the solution of $[\text{Cp}^*\text{RhCl}_2]_2$ (18.6 mg, 0.03 mmol) in methanol (6 mL) with stirring at room temperature for 5h. After filtration to remove AgCl, H_2pdt (8.6 mg, 0.06 mmol) in methanol (5 mL) treated by addition of MeONa (6.5 mg, 0.12 mmol) was mixed with the filtrate and stirred for 24h. Then the mixture was concentrated and extracted by dichloromethane to give a dark red solid, which was washed by diethyl ether and dried under vacuum. Yield: 8.5 mg, 30%. Crystals of **7** suitable for an X-ray diffraction study were obtained by slow diffusion of *n*hexane into dichloromethane. Anal. Calcd (%) for

$\text{C}_{43}\text{H}_{51}\text{N}_6\text{O}_3\text{S}_7\text{F}_3\text{AgRh}_3$: C 36.94, H 3.68, N 6.01. Found: C 36.89, H 3.65, N 5.95. IR (KBr disk): 2982(w), 2918(w), 1637(w), 1457(m), 1381(m), 1338(m), 1274(vs), 1245(vs), 1222(m), 1146(s), 1079(w), 1059(m), 1031(vs), 859(w), 753(w), 637(vs), 572(w), 517(w), 477(w), 454(w) cm^{-1} .

X-ray crystal structure determinations. All the determinations of unit cell and intensity data were performed with graphite-monochromated Mo $K\alpha$ radiation ($\lambda = 0.71073 \text{ \AA}$). All The data were collected at 173(2) or 193(2) K using the ω scan technique. These structures were solved by direct methods, using Fourier techniques, and refined on F_2 by a full-matrix least-squares method. All the calculations were carried out with the SHELXTL program.¹⁷ Crystal data, data collection parameters, and the results of the analysis of these complexes are listed in **Table 1**.

Table 1 Crystallographic data for complexes **1** and **3-7**.

	1	3	4	5	6	7
formula	$\text{C}_{28}\text{H}_{34}\text{N}_4\text{Rh}_2\text{S}_4$	$\text{C}_{14}\text{H}_{17}\text{IrN}_2\text{S}_2$	$\text{C}_{84}\text{H}_{94}\text{N}_4\text{O}_{20}\text{S}_8\text{Cl}_4\text{F}_{12}$ $\text{Rh}_6 \cdot 2\text{CH}_3\text{OH} \cdot \text{Et}_2\text{O}$	$\text{C}_{84}\text{H}_{94}\text{N}_4\text{O}_{20}\text{S}_8\text{Cl}_4\text{F}_{12}$ $\text{Ir}_6 \cdot 2\text{CH}_3\text{OH} \cdot \text{Et}_2\text{O}$	$\text{C}_{88}\text{H}_{98}\text{N}_6\text{O}_{20}\text{S}_8\text{Cl}_4\text{F}_{12}$ $\text{Rh}_6 \cdot 5\text{CH}_3\text{OH} \cdot 2\text{Et}_2\text{O} \cdot \text{H}_2\text{O}$	$\text{C}_{43}\text{H}_{51}\text{N}_6\text{O}_3\text{S}_7\text{F}_3\text{Ag}$ $\text{Rh}_3 \cdot 3\text{CH}_3\text{OH} \cdot \text{C}_6\text{H}_{12}$
<i>Mr</i>	760.66	469.64	2861.60	3397.49	3129.95	1578.21
crystal system	Monoclinic	Orthorhombic	Monoclinic	Monoclinic	Monoclinic	Orthorhombic
space group	$P 2_1/c$	$P c a 2_1$	$P 2_1/c$	$P 2_1/c$	$C 2/c$	$P b c n$
<i>a</i> [\AA]	15.9143(19)	16.4804(18)	13.8710(9)	13.9252(13)	29.239(4)	25.2150(14)
<i>b</i> [\AA]	14.3411(18)	13.5952(15)	26.3536(17)	26.276(3)	15.984(2)	16.4859(10)
<i>c</i> [\AA]	13.2230(16)	13.7037(15)	15.6676(11)	15.7341(15)	29.109(4)	28.9810(17)
α [$^\circ$]	90	90	90	90	90	90
β [$^\circ$]	98.709(2)	90	98.0260(10)	97.805(2)	110.880(2)	90
γ [$^\circ$]	90	90	90	90	90	90
<i>V</i> [\AA^3]	2983.1(6)	3070.4(6)	5671.2(7)	5703.8(9)	12711(3)	12047.2(12)
<i>T</i> [K]	193(2)	173(2)	173(2)	173(2)	173(2)	193(2)
<i>Z</i>	4	8	2	2	4	8
ρ_{calcd} [g cm^{-3}]	1.694	2.032	1.676	1.978	1.636	1.740
μ [mm^{-1}]	1.412	8.957	1.180	7.298	1.064	1.432
<i>F</i> (000)	1536	1792	2876	3260	6344	6384
Independent reflections	0.0523	0.0313	0.0392	0.0397	0.0427	0.0649
[<i>R</i> (int)]						
data/restraints/ parameters	6442/0/354	6484/1/353	12963/120/628	12030/175/625	13772/237/801	12532/20/538
R_1/wR_2 [$I > 2\sigma(I)$] ^a	0.0455/0.1233	0.0237/0.0511	0.0604/0.1793	0.0566/0.1676	0.0911/0.2416	0.0558/0.1459
R_1/wR_2 (all data) ^a	0.0760/0.1667	0.0310/0.0539	0.0843/0.1959	0.0766/0.1848	0.1280/0.2833	0.0927/0.1609
goodness-of-fit	1.066	1.002	1.031	1.066	1.048	0.944
largest residuals [$e \text{ \AA}^{-3}$]	1.580/-1.259	1.990/-0.958	2.765/-1.605	3.704/-2.855	2.978/-2.615	0.968/-0.735
ρ_{calcd} [g cm^{-3}]	1.694	2.032	1.676	1.978	1.636	1.740
μ [mm^{-1}]	1.412	8.957	1.180	7.298	1.064	1.432

[a] $R_1 = \sum ||F_o| - |F_c||$ (based on reflections with $F_o^2 > 2\sigma F_o^2$); $wR_2 = \{ \sum [\omega(F_o^2 - F_c^2)^2] / \sum [\omega(F_o^2)^2] \}^{1/2}$; $w = 1/[\sigma^2 F_o^2 + (0.095P)^2]$; $P = [\max(F_o^2, 0) + 2F_c^2]/3$ (also with $F_o^2 > 2\sigma F_o^2$).

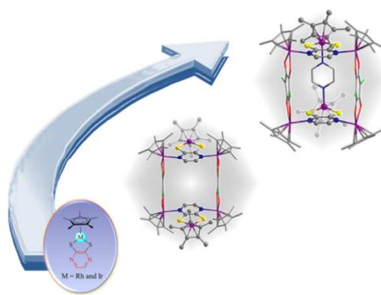
Acknowledgements

This work was supported by the National Science Foundation of China (21374019), the Program for Changjiang Scholars and Innovative Research Team in University (IRT1117), the National Basic Research Program of China (2015CB856600) and the Shanghai Science Technology Committee (13JC1400600, 13DZ2275200).

References

- (a) K. Ray, E. Bill, T. Weyhermüller and K. Wieghardt, *J. Am. Chem. Soc.*, 2005, **127**, 5641; (b) S. Takaishi, M. Hosoda, T. Kajiwara, H. Miyasaka, M. Yamashita, Y. Nakanishi, Y. Kitagawa, K. Yamaguchi, A. Kobayashi and H. Kitagawa, *Inorg. Chem.*, 2009, **48**, 9048; (c) T. Kusamoto, S. Kume and H. Nishihara, *Angew. Chem. Int. Ed.*, 2010, **49**, 529; (d) W. R. Mcnamara, Z. Han, P. J. Alperin, W. W. Brennessel, P. L. Holland and R. Eisenberg, *J. Am. Chem. Soc.*, 2011, **133**, 15368; (e) F. Shojaei, J. R. Hahn and H. S. Kang, *Chem. Mater.*, 2014, **26**, 2967.
- (a) B. L. Davis, D. A. Dixon, E. B. Garner, J. C. Gordon, M. H. Matus, B. Scott and F. H. Stephens, *Angew. Chem., Int. Ed.*, 2009, **48**, 6812; (b) R. K. M. Khan, S. Torke and A. H. Hoveyda, *J. Am. Chem. Soc.*, 2013, **135**, 10258; (c) S. Pullen, H. Fei, A. Orthaber, S. M. Cohen and S. Ott, *J. Am. Chem. Soc.*, 2013, **135**, 16997; (d) Y.-F. Han and G.-X. Jin, *Acc. Chem. Res.*, 2014, **47**, 3571; (e) H.-X. Li, E. N. Brothers and M. B. Hall, *Inorg. Chem.*, 2014, **53**, 9679.
- (a) K. Osakada, Y. Kawaguchi and T. Yamamoto, *Organometallics*, 1995, **14**, 4542; (b) M. Fourmigue, *Coord. Chem. Rev.*, 1998, **178-180**, 823; (c) M. Herberhold, G.-X. Jin, H. Yan, W. Milius and B. Wrackmeyer, *Eur. J. Inorg. Chem.*, 1999, 873; (d) M. Nihei, T. Nankawa, M. Kurihara, and H. Nishihara, *Angew. Chem., Int. Ed.*, 1999, **38**, 1098.
- (a) W.-F. Liaw, C.-K. Hsieh, G.-Y. Lin and G.-H. Lee, *Inorg. Chem.*, 2001, **40**, 3468; (b) S. Liu, Y.-F. Han and G.-X. Jin, *Chem. Soc. Rev.*, 2007, **36**, 1543; (c) K. Baba, T. A. Okamura, H. Yamamoto, T. Yamamoto and N. Ueyama, *Inorg. Chem.*, 2008, **47**, 2873; (d) P. Chandrasekaran, A. F. Greene, K. Lillich, S. Capone, J. T. Mague, S. DeBeer and J. P. Donahue, *Inorg. Chem.*, 2014, **53**, 9192.
- (a) S. Liu, G.-L. Wang and G.-X. Jin, *Dalton Trans.*, 2008, 425; (b) T. Kambe, R. Sakamoto, T. Kusamoto, T. Pal, N. Fukui, K. Hoshiko, T. Shimojima, Z.-F. Wang, T. Hirahara, K. Ishizaka, S. Hasegawa, F. Liu, and H. Nishihara, *J. Am. Chem. Soc.*, 2014, **136**, 14357.
- (a) F. E. Hahn, B. Birkmann and T. Pape, *Dalton Trans.*, 2008, 2100; (b) B.-H. Zhu, Y. Shibata, S. Muratsugu, Y. Yamanoi and H. Nishihara, *Angew. Chem. Int. Ed.*, 2009, **48**, 3858; (c) F. Hupka and F. E. Hahn, *Chem. Commun.*, 2010, **46**, 3744; (d) A. F. Furcate, N. Bellec, O. Jeannin, P. A. Senzier, M. Fourmigué, A. Vacher and D. Lorcy, *Inorg. Chem.*, 2014, **53**, 8681; (e) A. J. Clough, J. W. Yoo, M. H. Mecklenburg and S. C. Marinescu, *J. Am. Chem. Soc.*, 2015, **137**, 118.
- (a) T. Kreickmann, C. Diedrich, T. Pape, H. V. Huynh, S. Grimme and F. E. Hahn, *J. Am. Chem. Soc.*, 2006, **128**, 11808; (b) T. R. Johannessen, K. Schenk and K. Severin, *Inorg. Chem.*, 2010, **49**, 9546; (c) A. Granzhan, C. Schouwey, T. R. Johannessen, R. Scopelliti and K. Severin, *J. Am. Chem. Soc.*, 2011, **133**, 7106; (d) C.-F. Zhu, G.-Z. Yuan, X. Chen, Z.-W. Yang and Y. Cui, *J. Am. Chem. Soc.*, 2012, **134**, 8058; (e) T. R. Cook, Y. R. Zheng and P. J. Stang, *Chem. Rev.*, 2013, **113**, 734; (f) T. R. Cook, V. Vajpayee, M. H. Lee, P. J. Stang and K.-W. Chi, *Acc. Chem. Res.*, 2013, **46**, 2464.
- (a) F. E. Hahn, C. S. Isfort and T. Pape, *Angew. Chem. Int. Ed.*, 2004, **43**, 4807; (b) T. Kreickmann and F. E. Hahn, *Chem. Commun.*, 2007, 1111; (c) F. E. Hahn, M. Offermann, C. S. Isfort, T. Pape and R. Fröhlich, *Angew. Chem. Int. Ed.*, 2008, **47**, 6794; (d) B. Birkmann, R. Fröhlich and F. E. Hahn, *Chem. - Eur. J.*, 2009, **15**, 9325.
- (a) X.-B. Xi, Y. Fang, T.-W. Dong and Y. Cui, *Angew. Chem. Int. Ed.*, 2011, **50**, 1154; (b) T. Kambe, R. Sakamoto, K. Hoshiko, K. Takada, M. Miyachi, J. H. Ryu, S. Sasaki, J. Kim, K. Nakazato, M. Takata and H. Nishihara, *J. Am. Chem. Soc.*, 2013, **135**, 2462; (c) S.-S. Bao, K. Otsubo, J. M. Taylor, Z. Jiang, L.-M. Zheng and H. Kitagawa, *J. Am. Chem. Soc.*, 2014, **136**, 9292.
- (a) X. Ribas, J. Dias, J. Morgado, K. Wurst, M. Almeida, J. Veciana and C. Rovira, *CrystEngComm*, 2002, **4(93)**, 564; (b) X. Ribas, J. C. Dias, J. Morgado, K. Wurst, E. Molins, E. Ruiz, M. Almeida, J. Veciana and C. Rovira, *Chem. - Eur. J.*, 2004, **10**, 1691; (c) Y. Kobayashi, B. Jacobs, M. D. Allendorf and J.-R. Long, *Chem. Mater.*, 2010, **22**, 4120; (d) S. Takaishi, N. Ishihara, K. Kubo, K. Katoh, B. K. Breedlove, H. Miyasaka, and M. Yamashita, *Inorg. Chem.*, 2011, **50**, 6405.
- (a) D. Sellmann, M. Geck, F. Knoch, G. Ritter and J. Dengler, *J. Am. Chem. Soc.*, 1991, **113**, 3819; (b) R. Xi, M. Abe, T. Suzuki, T. Nishioka and K. Isobe, *J. Organomet. Chem.*, 1997, **549**, 117; (c) M. Herberhold, H. Yan, W. Milius and B. Wrackmeyer, *Chem. - Eur. J.*, 2000, **6**, 3026; (d) W. F. Liaw, C. K. Hsieh, G.-Y. Lin and G. H. Lee, *Inorg. Chem.*, 2001, **40**, 3468; (e) S. Tsukada, Y. Shibata, R. Sakamoto, T. Kambe, T. Ozeki and H. Nishihara, *Inorg. Chem.*, 2012, **51**, 1228.
- (a) Y.-F. Han, W.-G. Jia, Y.-J. Lin and G.-X. Jin, *Angew. Chem., Int. Ed.*, 2009, **48**, 6234; (b) S.-L. Huang, Y.-J. Lin, T. S. A. Hor and G.-X. Jin, *J. Am. Chem. Soc.*, 2013, **135**, 8125; (c) Y.-F. Han and G.-X. Jin, *Chem. Soc. Rev.*, 2014, **43**, 2799.
- (a) Y.-F. Han, W.-G. Jia, W.-B. Yu, Y.-J. Lin and G.-X. Jin, *Chem. Soc. Rev.*, 2009, **38**, 3419; (b) Y.-F. Han, H. Li, Z.-F. Zheng and G.-X. Jin, *Chem. Asian J.*, 2012, **7**, 1243.
- (a) T. Suzuki, A. G. Dipasquale and J. M. Mayer, *J. Am. Chem. Soc.*, 2003, **125**, 10514; (b) K. D. Hesp, R. McDonald, M. J. Ferguson and M. Stradiotto, *J. Am. Chem. Soc.*, 2008, **130**, 16394; (c) S. Muratsugu, K. Sodeyama, F. Kitamura, M. Sugimoto, S. Tsuneyuki, S. Miyashita, T. Kato and H. Nishihara, *J. Am. Chem. Soc.*, 2009, **131**, 1388; (d) Y.-F. Han, L. Zhang, L.-H. Weng and G.-X. Jin, *J. Am. Chem. Soc.*, 2014, **136**, 14608.
- (a) S. H. Gellman, G. P. Dado, G.-B. Liang and B. R. Adams, *J. Am. Chem. Soc.*, 1991, **113**, 1164; (b) S. Habe, T. Yamada, T. Nankawa, J. Mizutani, M. Murata and H. Nishihara, *Inorg. Chem.*, 2003, **42**, 1952; (c) G. E. Garrett, G. L. Gibson, R. N. Straus, D. S. Seferos and M. S. Taylor, *J. Am. Chem. Soc.*, 2015, **137**, 4126.
- (a) M. A. Bennett, T.-N. Huang, T. W. Matheeson and A. K. Smith, *Inorg. Synth.*, 1982, **21**, 74; (b) C. White, A. Yates and P. M. Maitlis, *Inorg. Synth.*, 1992, **29**, 228.
- Sheldrick, G. M. SHELXL-97; Universität Göttingen: Germany, 1997.

Toc Graphic



Text:

The coordinatively unsaturated 16-electron half-sandwich precursors $[\text{Cp}^*\text{M}(\text{pdt})]$ ($\text{M} = \text{Rh}$ and Ir , $\text{pdt} = \text{pyrazine-2,3-dithiol}$) have been synthesized. Utilizing their bridging and unsaturated attributes, and further used in stepwise assembly reactions with the binuclear blocks to give closed molecular box.